USE OF LIQUID FILM EVAPORATION IN BIPOROUS MEDIA TO ACHIEVE HIGH HEAT FLUX OVER LARGE AREAS

Tadej Semenic, Ying Yu Lin, Ivan Catton
Morrin, Martinelli, Gier Memorial Heat Transfer Laboratory
Department of Mechanical and Aerospace Engineering
School of Engineering and Applied Science
University of California, Los Angeles
Los Angeles, CA 90095-1597
Tel. 310-825-8185; Email: catton@ucla.edu

David B. Sarraf
Advanced Cooling Technologies, Inc.
1046 New Holland Avenue
Lancaster, PA 17601
Tel. 717-295-6059; Email: dave.sarraf@1-ACT.com

Abstract

Three monoporous wicks with average powder diameters 60, 300 and 600 μm and five biporous wicks with average cluster (μm) to powder (μm) ratios and wick thickness (mm) 600/60/4, 300/60/4, 600/40/1, 300/60/1 and 300/40/1 were tested with distilled water. Dryout for monoporous wicks were: 223 W/cm^2 at 37 °C superheat (60 μm), 209 W/cm^2 at 31 °C superheat (600 μm), and 222 W/cm^2 at 73 °C superheat (300 μm). Dryout for biporous wicks were 236.5 W/cm^2 at 45 °C superheat (300/40/1), 160 W/cm^2 at 18 °C superheat (600/40/1), and 150 W/cm^2 at 32.5 °C superheat (300/60/1). Dryout for thick wicks were not seen. They were able to remove 202 W/cm^2 at 81°C superheat (300/60/4) and 494 W/cm^2 at 128 °C superheat (600/60/4). The 300/40/1 wick showed the highest heat transfer coefficient, 10.4 W/(cm^2 K), at 180 W/cm^2. For high heat flux removal is most desired 600/60/4 wick, which can continuously remove heat at almost constant heat transfer coefficient, 4.2 W/(cm^2·K), without seeing a dryout. All wicks were tested at a partial pressure of the water vapor 0.1 atm.

KEYWORDS

Bidispersed, biporous, high heat fluxes, electronic cooling.

INTRODUCTION

High voltage power electronics, some laser diode arrays can generate heat fluxes of more then 100 W/cm^2. In some MOSFET or IGBT chips, peak heat fluxes can reach 1 kW/cm^2 [1]. Heat pipes with sintered powder wicks can tolerate heat fluxes up to 80 W/cm^2 [2]. There are two factors that limit maximum heat flux that can be removed with a heat pipe, they are: capillary and boiling limit. Capillary limit occurs when the capillary pressure formed at liquid vapor interfaces of the menisci in the porous wick is lower then sum of the pressure drops along the fluid circulation path. Boiling limit occurs when the vapor generated at hot spots of the wick is trapped due to geometry limitations.

Several authors have offered novel structures with separations of liquid and vapor phases. Liter and Kaviany [3] were able to enhance pool-boiling critical heat flux nearly three times over that of a plain surface using modulated (periodically non-uniform thickness) porous layer coatings. The wick structure was able to separate liquid and vapor phases and therefore reduced the vapor counterflow resistance. Zuo and North [4] were able to dissipate 200W/cm^2 with graded wick transport mechanism (GWT). GWT is a porous sintered wick that consists of a fine powder wick for capillary pumping and a coarse powder wick for liquid transportation. Two different arrangements were tested. First one had the fine powder wick sintered above the heat source and the second one had the fine powder wick sintered on the top of the course one. Vityaz et al [5] oxidized sintered copper wick and this way formed two level structure, a biporous wick, which was able to remove five times more heat then non-oxidized one. Oxide on the surface of copper powder formed micropores with strong capillary suction while the macropores between the powder allowed and easy escape of the vapor.

North at al [6] formed a bidispersed structure with sintering together clusters made of copper powder. Micropores between powder were able to continuously supply the working fluid to voids

between clusters where the thin film evaporation took place. They were able to remove six times more heat with a biporous wick than with a comparable monoporous. Cao at al [7] tested two monodispersed copper wicks with powder sizes 103 μm and 1986 μm, and three bidispersed copper wicks with cluster (μm) to powder (μm) ratios 334/103, 815/103, and 1986/103 at three different adverse hydrostatic heads. Correlation for monoporous sintered copper given in Lin at al [8] was used to convert pore diameters to powder diameters. They found that the 815/103μm bidispersed wick performs best. It was able to remove 85 W/cm^2 at temperature difference 12°C and the smallest adverse pressure head. North at all [10] tested monodispersed nickel wick with powder size 400 μm, bidispersed nickel wick with cluster (μm) to powder (μm) ratio 400/70 and two bidispersed copper wicks with cluster (μm) to powder (μm) ratios 600/80 and 420/70. All wicks were 0.65 mm thick. Best performed bidispersed copper wick with largest clusters, second best was bidispersed nickel wick. Dryout for 400/70 bidispersed nickel occurred at 80 W/cm^2 and 20 °C temperature difference and the dryout for 600/80 bidispersed copper at 70 W/cm^2 and 10 °C temperature difference. Even though the dryout for bidispersed nickel occurred at higher heat flux, the superheat was twice as high then for the bidispersed copper.

Wang and Catton [1] developed an evaporation-boiling evaporation (EBE) model for predicting critical heat fluxes of biporous wicks. The model predicted 3kW/cm^2 heat removal at superheat of 30 °C when using 4-mm thick biporous copper wick with cluster (μm) to powder (μm) ratio 300/80.

In present work three monoporous wicks with average powder sizes 60, 300 and 600 μm and five biporous wicks with average cluster(μm)/powder(μm) ratios and thickness(mm) 300/60/4, 300/60/1, 600/40/1, 300/40/1, and 600/60/4 are sintered from oxygen free copper at temperatures 900-1000 ° and tested with distilled water. Heat flux into boiling region was calculated using Furrier's law and interface wall wick temperature determined. Boiling curves for all the wicks were plotted and the dryout points of the wicks compared. Objective of this work is to first show the advantages of biporous sintered wick and second to relate the wick dryout to the wick geometry. We are searching for a wick geometry (cluster size, powder size, wick thickness) that will remove the highest heat flux at still acceptable interface temperature.

EXPERIMENTAL APPARATUS

Table 1 shows powder diameter ranges and thermophysical properties of monoporous wicks. At this point thermophysical properties of biporous wicks are still being measured.

Table 1. Thermophysical Properties of Monoporous Wicks from Lin at al [8]

Powder Size (μm)	Porosity	Permeability (Darcy's)	Capillary Pressure(Pa)	Thermal Conductivity(W/(m·K))
32.5-44	31.5	0.34	9604.3	209
53-63	31.8	1.08	3422.4	189
250-354	34.5	44.84	1606.6	109
500-710	33.6	130.58	882.7	143

Powder distributions for the wicks tested is in all cases Gaussian distribution. Particle shapes are spherical or spheroidal. This morphology coupled with a narrow band distribution explains low porosity. Ordinary angular powder with a wide distribution results typically results in porosities 45-55%.

Experimental apparatus consists of a heat pipe made of oxygen free copper, a wick that is being tested and a heater (Figure 1). The copper base of the heat pipe was brazed to the copper cylinder. Sight glass was attached to the unit to allow a precise control of the charge. Heater was made of copper block and three 750 W, 3"long, 0.5"diameter cartridge heaters. Negative tolerances were used to assure low thermal resistance between the cartridges and the copper block. Temperature of the present heater is limited to 950°C. Wicks were sintered on a copper base (boiling target). The boiling target with a wick on the top was soldered to the heater and sealed to the boiling apparatus with a silicon o-ring and six screws. Temperatures inside the boiling target were monitored at several places as shown with red dots (circles) in Figure 2.

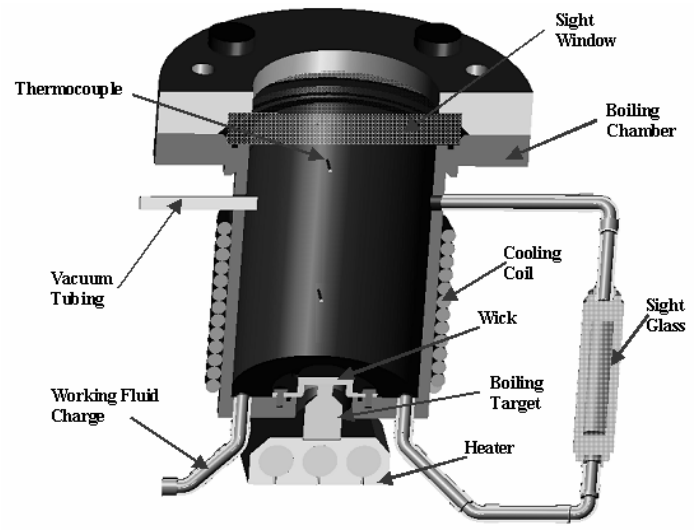

Fig. 1. Heat Pipe for Testing Sintered Wicks

The diameter of the wick is 5.7 cm. Only a central region of the wick is a boiling region (diameter 0.95 cm). The purpose of the outside part of the wick is to feed the working liquid into the boiling region. This particular geometry also allows monitoring temperatures below the wick for calculating radial heat losses. The ratio of the radial heat losses over the total input heat gives an indication of dryout inside thick wicks (a minimum heat flux appears at CHF).

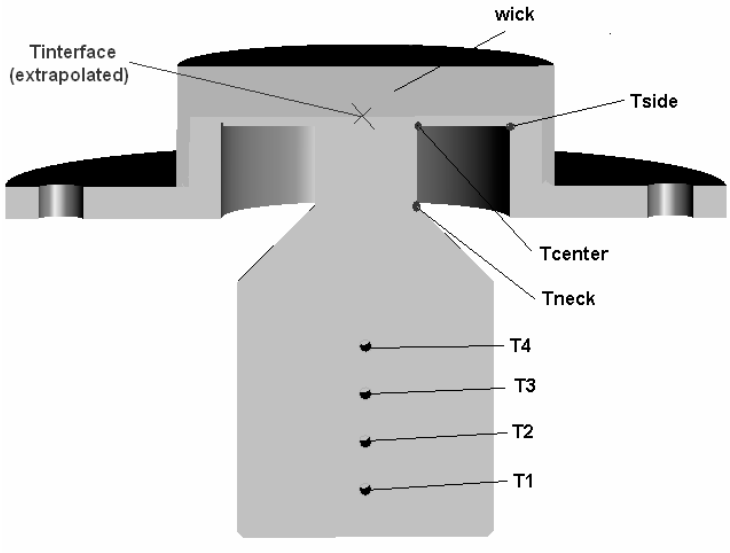

Fig. 2. Boiling Target

The heater and the boiling target were insulated with silica blanket (thermal conductivity 0.02 W/m·K). Temperatures inside the boiling chamber were measured are three locations: right above the wick, below the sight window and at the wall of the chamber (condenser temperature). During the operation, circulation water was pumped at a constant flow rate through the cooling coil. The temperature of the circulating water was digitally controlled and heated with high power cartridge heater or cooled with cooling water from another loop as needed. The sight window allowed an optical access to the top of the wick surface, which was essential to verify liquid level to see the nucleation and the dryout.

EXPERIMENTAL PROCEDURE

A wick was placed inside the boiling chamber; the boiling chamber was closed and evacuated. The heater was set to a high heat flux (right below the CHF) and let run for approximately an hour to remove as much air as possibly from the pores. While heating, the chamber was evacuated several

times. Cooling water temperature was set to (40±0.5)°C and kept constant during the experiment. When both thermocouples read the same vapor temperature (±0.1°C) and the wall temperature reads a slightly lower temperature, it was assumed that only a small amount of air remains in the chamber. A significant amount of air would cause several degree temperature drop between condenser and vapor temperature. Once most of the air was removed from the test chamber, the power to the heater was adjusted to approximately 20 W/cm^2.

After the steady state was achieved, the pressure inside the chamber was 0.08atm. Heat being supplied to the heater was gradually increased and data taken at several steady state power levels until the dryout was seen. Steady state was achieved in about 20 minutes. Temperatures were recorded for approximately 10 minutes. Temperatures T1 and T4 (Figure 2) were set as boundary conditions in a Final Element Analysis Method to predict interface wall/wick temperature. Interface temperature was also extrapolated using T_{neck} and T_{center} temperature readings and calculated assuming a constant heat resistance for the given geometry at applied heat 1 W. Thermocouple readings T_{center} and T_{side} were used to estimate radial heat flux inside the copper collar. Temperatures at the center of the copper collar were assumed to be arithmetic averages between T_{center} (T_{side}) and the vapor temperature. Radial heat flux was calculated from steady conduction inside a copper disk.

The net heat flux supplied to the boiling region was calculated as heat flux calculated from temperatures T1 and T4 using Fourier's law minus radial heat flux in the collar. The radial heat flux inside the wick was neglected due to a much lower thermal conductivity of the wick comparing to pure copper. Thermal conductivity of the copper was taken to be 401 at 300 K and 393 at 400 K. At each heat flux a linearity of the temperatures T1 through T4 was checked.

RESULTS AND DISCUSSION

Figure 3 shows boiling curves for monoporous wicks.

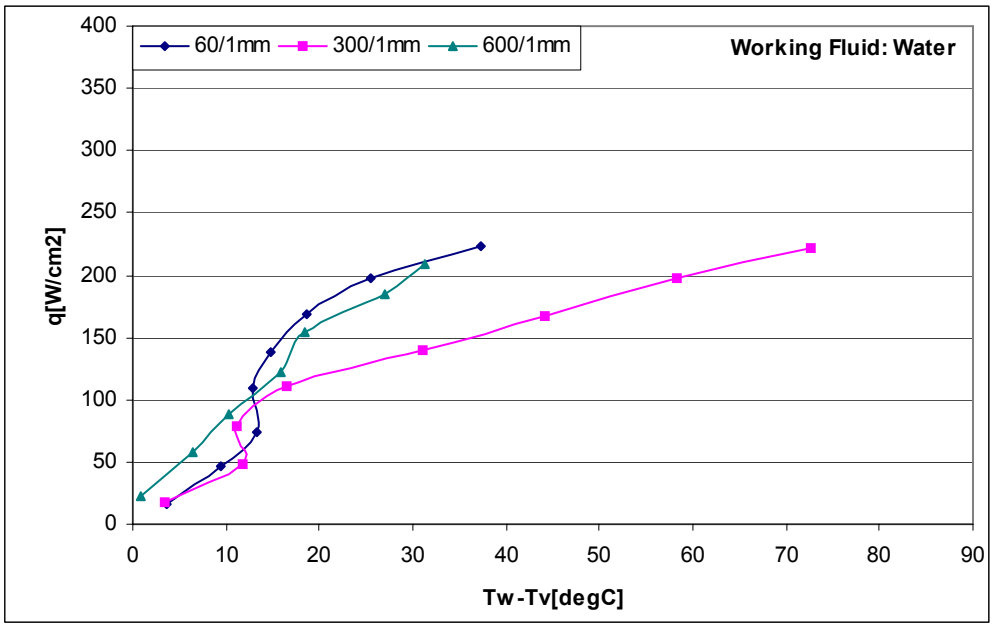

Fig. 3. Boiling Curves for Monoporous Wicks

In Figures 3 and 4, powder size 60μm is for the distribution 53-63 μm, 300 μm for 250-354 μm and 600 μm for 500-710 μm.

Result analysis showed the highest heat transfer coefficient, 9.35 W/cm^2·K, at 138 W/cm^2 for wick with average powder diameter 60 μm. Dryout for this wick was at 223 W/cm^2 and superheat 37.3°C. Second highest heat transfer coefficient, 8.61W/cm^2·K, at 88W/cm^2 had wick with average powder size 600 μm. Dryout appeared at 209.5 W/cm^2 and 31.2°C superheat. The lowest heat transfer coefficient, 7 W/cm^2·K, at 79 W/cm^2 was measured for the wick with 300 μm average powder size. Dryout for this wick was at 222.4 W/cm^2 and superheat 73°C.

Looking at the thermophysical properties in Table 1 and boiling curves on Figure 3, we can see that as powder size becomes smaller, the permeability becomes lower; on the other hand, the thermal conductivity and capillary pressure becomes higher. The best performs a wick with the smallest powder size and therefore, highest capillary suction and highest thermal conductivity, second best is wick with the largest powder size and therefore, highest permeability, medium high thermal conductivity, and smallest capillary pressure. The worst performed the wick with the medium powder diameter, the lowest thermal conductivity, medium high permeability and medium high capillary pressure.

Now lets take a look at the performances of the biporous wicks, see Figure 4.

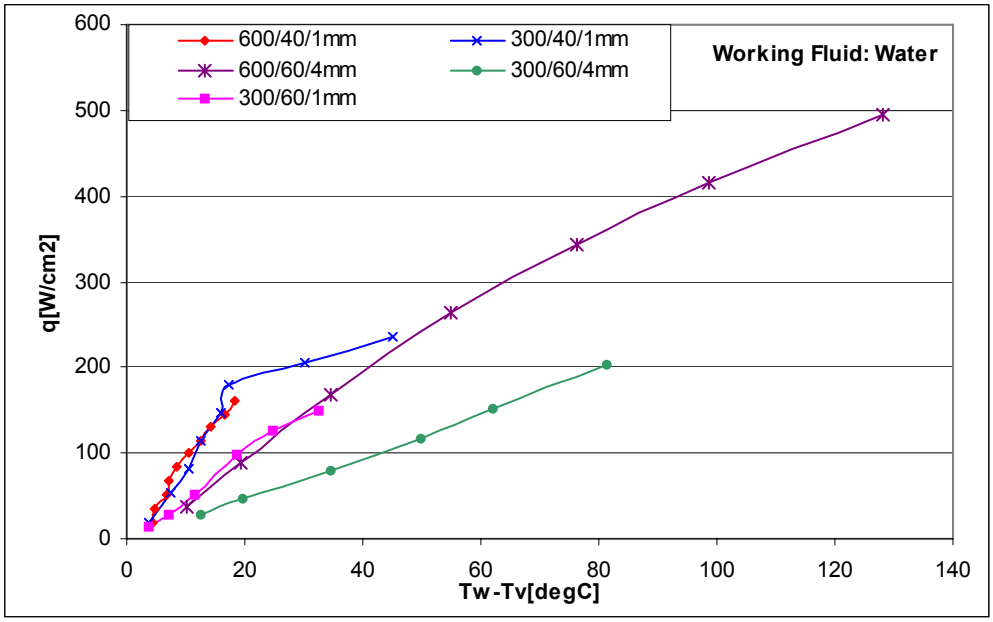

Fig. 4. Boiling Curves for Biporous Wicks

From data analysis it was seen that 300/40/1 biporous wick dried out at 236.5 W/cm^2 and superheat 45 °C. The highest heat transfer coefficient, 10.4 (W/cm^2·K), was seen at 180 W/cm^2. Second highest heat transfer coefficient, 9.8 W/(cm^2·K), was seen at 600/40/1 wick (heat flux 85 W/cm^2). The dry out for this wick started at 160 W/cm^2 and 18 °C. It is believed that this wick has higher capabilities. Third largest heat transfer coefficient, 5.4 (W/cm^2·K) was developed at 100 W/cm^2 at 300/60/1 wick. This wick dried out at 150 W/cm^2 and 32.5 °C. Following are results for the two thick wicks. For these two wicks the dryout was not seen from the top of the wick. It is assumed to appear inside the wick while the working liquid was still supplied from the top. The highest heat transfer coefficient for 600/60/4 wick was 5 (W/cm^2·K) and it was measured at 170 (W/cm^2). The wick was able to remove 494 W/cm^2 at 128 °C superheat. Interface temperature in this case was 200 °C. Heat was seen to be removed continuously at an average heat transfer coefficient 4 (W/cm^2·K). The last thick wick, 300/60/4, showed the highest heat transfer coefficient, 2.5 (W/cm^2·K), at 202 W/cm^2 and superheat 81 °C. This was also the highest measured heat flux for this wick.

Nucleation for all the wicks was at heat fluxes from 17-22 W/cm^2 and temperature differences 4-5 °C. Chen at all [9] measured permeabilities for biporous and monoporous wicks and they concluded that the permeabilities of monoporous wicks with the same powder size as the cluster size of biporous wicks are equal. For the capillary pressure of biporous wicks, we can assume that as powder and cluster sizes get smaller, the capillary pressure becomes bigger. From Figure 4, we can see that for heat fluxes below 130 W/cm^2 600/40/1 wick performs best. From 130-250 W/cm^2 performs best 300/40/1 wick and for higher heat fluxes then 250 W/cm^2, 600/60/4 wick. Comparing 600/60/4 wick with 300/60/4 wick, we can see that it is beneficial to have larger clusters. The difference is less obvious when comparing 600/40/1 and 300/40/1 wicks. When comparing 300/60/1 wick with 300/40/1, we can see that it is better to have powder with smaller diameter. Thick wick is able to remove more heat then a thin one without seeing a dryout; however, the superheat gets very high. The 1-mm thick wicks were all completely dry at heat fluxes above 250 W/cm^2. In order to remove heat

fluxes higher then 250 W/cm^2 at not too high interface temperature, a thick wick with enough spacing between clusters and still high capillary pressure is desired. Figure 5 shows SEM photograph of a 600/60/4 wick. We can see that clusters are not nice spheres as and in many cases they appear to block the vapor passages.

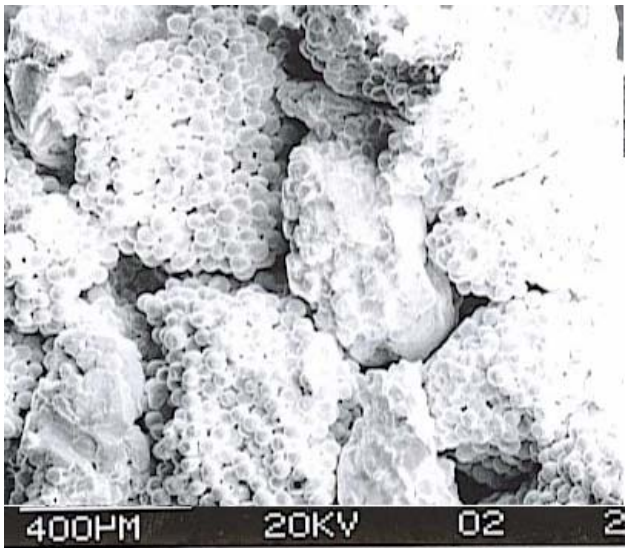

Fig. 5. SEM Photograph of the 600/60 Biporous Wick

While running the experiment it was seen that vapor escaped from the wick at no more then 3 to 5 places. We concluded that only 3-5 vapor columns were formed. More symmetrical clusters are desired for an easier escape of the vapor. We can assume that much higher superheat then predicted in [1] is a result of non-ideal vapor passages.

UNCERTAINTY ANALYSIS

Temperatures were recorded at steady state. Steady state was chosen to be reached when the temperature did not rise for more the 0.5 °C in 15minutes. 165 temperature readings were averaged to get an average temperature. Standard deviation was less then 0.1 °C. Linearity of temperatures T1 to T4 was found to be 0.9 to 0.98. Temperature differences T1-T2, T2-T3, T3-T4 at low heat fluxes were differed by as much as 15% and as heat flux became higher the differences eventually became equal.

The same amount of insulation was always used to insulate the heater and the target. Approximately 90% of the supplied power went to the boiling target and from this heat approximately 70-80% went into the boiling region. The rest, 20-30%, was radially conducted into the collar. Radial heat losses were measured for each case separately.

Total error in measuring net heat fluxes is estimated to be around 5%. Most of the error comes from the estimation of the radial heat losses. Interface temperature was extrapolated using T_{neck} and T_{center} temperature readings, and it compares within 1% to FEM predictions.

Vapor temperatures were not different for more then 0.2 °C. It is estimated that approximately 1% of the air was still left in the chamber. While running experiments pressure was monitored and using steam tables the saturation temperature was calculated. For all 1mm thick wicks, the vapor temperature rose from 40-48 °C as the heat was increased. Vapor temperatures compares within 1 °C to the saturation temperature. Larger difference was seen at lower heat fluxes and almost no difference at higher heat fluxes. The condenser temperature was always approximately 0.5 °C below the vapor temperature to drive the vapor toward the condenser.

CONCLUSIONS

A biporous wick was shown to perform better then an equivalent monoporous wick. This demonstrates the concept of flow separation. Even though the voids were filled with the vapor, the working fluid was still supplied to the hot spots through micropores inside the clusters. Bigger clusters were found to

perform better when comparing two thick wicks. Even though there is already a dry region inside the thick wick it is still able to remove heat at almost constant heat transfer coefficient. The highest heat flux, 494 W/cm^2, was removed with 600/60/4 mm wick at temperature difference of 128 °C. It is assumed that the same heat flux can be removed with much lower superheat if cluster would be more symmetrical.

ACKNOWLEDGEMENTS

The authors would like to acknowledge the support of U.S. Navy/ Office of Naval Research with Dr. Mark Spector as program manager. The grant award number is N00014-04-1-0280.

References

1. Wang J., Catton I. Vaporization Heat Transfer in Biporous Wicks of Heat Pipe Evaporators // *Proc. 13th International Heat Pipe Conference,* Vol. 2, pp. 76-86, 2004.
2. Gopal M.R., Murthy S.S. Prediction of heat and mass transfer in annular cylindrical metal hydride beds // *Intl J. Hydrogen Energy*. 1992. Vol. 17. Pp. 795-805.
3. Thema-Base™ Heat Sink Application Notes, Thermacore, Inc, 1999.
4. Liter S., G., Kaviany M., Pool-boiling CHF enhancement by modulated porous-layer coating: theory and experiment // *Int. J. Heat Mass Transfer*. 2001. Vol. 44. Pp. 4287-4311.
5. Zuo Z.J., North M.T. Miniature high heat flux heat pipes for cooling of electronics, Thermacore, Inc., 1999.
6. Vityaz P.A., Konev S.K., Medvedev V.B., Sheleg V.K. Heat pipes with bidispersed capillary structures // *Proc. 5th International Heat Pipe Conference*, Vol. 1. Pp.127-135. 1984.
7. North M., T., Sarraf D.B., Rosenfeld J.H., Maidanik Y.F., Vershinin S. High heat flux loop heat pipes // *Proceedings of the Sixth European Symposium on Space Enviromental Control Systems*, Noordwijk, The Netherlands, 20-22 May 1997.
8. Cao X.L., Cheng P., Zhao T.S. Experimental study of evaporative heat transfer in sintered copper bidispersed wick structures // *Journal of Thermophysics and Heat Transfer*. 2002. Vol. 16. No.4. Pp. 547-552.
9. Lin Y.Y., Semenic T., Catton I. Thermophysical properties of monoporous sintered wicks // In preparation for HT05, San Francisco, July 20-25. 2005.
10. Chen Z.Q., Cheng P., Zhao T.S. An experimental study of two phase flow and boiling heat transfer in bi-dispersed porous channels // *Int. Comm. Heat Mass Transfer*. 2000. Vol. 27, No. 3. Pp. 293-302.
11. North M.T., Rosenfeld J.H., Shaubach R.M. Liquid film evaporation from bidisperse capillary wicks in heat pipe evaporators // *Proc. 9th International Heat Pipe Conference*, Albuquerque, NM, May 1-5, 1995.